International Journal on Advanced Science Engineering Information Technology

Vol.11 (2021) No. 3
ISSN: 2088-5334

# The Latowu Ultramafic Rock-Hosted Iron Mineralization in the Southeastern Arm Sulawesi, Indonesia: Characteristics, Origin, and Implication for Beneficiation

Sufriadin[a,*], Sri Widodo[a], Meinarni Thamrin[a], Akane Ito[b], Tsubasa Otake[b]

[a]*Department of Mining Engineering, Universitas Hasanuddin, South Sulawesi, Indonesia*
[b]*Division of Sustainable Resources Engineering, Graduate School of Engineering, Hokkaido University, Sapporo 060-8628, Japan*
*Corresponding author: *sufri.as@unhas.ac.id*

***Abstract*—Latowu ultramafic block in the Southeastern Arm Sulawesi locally hosts elevated concentrations of Fe in addition to Ni. We investigated both host rock and mineralized samples' mineralogy and chemistry to find out mineralogical and chemical characteristics and interpret the iron mineralization process with beneficiation implications. The mineralogical nature of the samples was analyzed using optical microscopy and X-ray diffractometry (XRD) methods. The whole-rock and mineral chemistry analyses were performed using X-ray fluorescence (XRF) spectroscopy and electron probe microanalysis (EPMA) techniques. The analysis showed that the ultramafic rocks had been undergone a strong to complete serpentinization degree where lizardite appears to be the predominant mineral. Magnetite in this research comprised the principal iron-bearing mineral and functioned as discrete fine-grains and subhedral to anhedral crystals. Magnetite occurs as fragments in breccia, alteration rim in spinel, fine-grained disseminations, and micro veins. This research found that the whole-rock chemistry of an ultramafic breccia showed an elevated concentration in $Fe_2O_3$ with a grade of 28.44 wt%. Electron probe analysis of magnetite shows a wide variation of Fe ranging from 31.10 wt% to 67.20 wt%. It is interpreted that the formation of magnetite within ultramafic rocks is influenced by the hydration of primary minerals, mainly olivine. Iron is most likely released from olivine or pyroxene crystals during serpentinization, and the higher water content of serpentine promotes its mobility. It is suggested that the magnetic separation method can be potentially used to increase the Fe grade.**

***Keywords*— Serpentine; ultramafic rocks; magnetite; iron ore; lizardite.**

*Manuscript received 31 Oct. 2019; revised 13 Dec. 2020; accepted 2 Feb. 2021. Date of publication 30 Jun. 2021.*


## I. INTRODUCTION

The steady increase of sponge iron demand as raw materials in iron and steel manufacturing has increased the effort to investigate the iron deposits from various sources. Australia, Brazil, and China are currently the major iron ore producing countries [1]. With the strongly depleted of conventional iron ore resources, mainly banded iron formation (BIF) from those countries, it is necessary to seek the iron resources in other *ore* sources, including from *lateritic ore* [2].

Although hematite is thought to be the predominant mineral containing in the iron ores, magnetite is also essential as an iron-bearing mineral because it can occur widespread in various types of bare igneous rocks, in the banded magnetite-quartzite formation, and also in titanomagnetite sand [3]. The ultramafic rocks have been reported as one of the igneous rock types that can host for iron ore deposit with economic value, such as found in the Cogne Magnetite Deposit of Italy [4, 5], Bau-Azzer ophiolite, Anti Atlas of Morocco [6], and the magnetite deposit of Oman Peridotite [7].

The occurrence of iron ore in association with an ultrabasic rock can be related to the serpentinization process, producing magnetite [8]. Serpentinization can also be accompanied by Ni-Cu rich minerals such as pentlandite, millerite, and chalcopyrite. The other significant changes that follow the serpentinization process are reducing density and increasing natural remanent magnetization (NRM) of ultramafic rock. The extent of serpentinization may control the texture, composition, and abundance of magnetite [9]. Therefore, the serpentinites' magnetic properties are affected by the mineral and chemical composition of parent rock and serpentinization degree of protolith [10].

The indication of ore mineral occurrences, mainly Ni sulfide mineralization hosted in the Latowu serpentinized ultramafic rocks, was first reported by reference [11]. However, iron-rich mineralization associated with this rock in this area has not been documented yet.

The objectives of this paper are (i) to describe and observe the petrological, mineralogical, and chemical nature of the ultramafic host rocks in the Latowu area, (ii) to characterize and analyze the properties of iron-bearing minerals associated with ultramafic host focusing on the occurrence and the origin of magnetite, (iii) to assess the processes responsible for iron mineralization, and (iv) to predict the suitable beneficiation method in upgrading the iron value.

## II. MATERIAL AND METHODS

### A. Geology and Sample Location

Latowu ultramafic block is located in the northwestern part of southeast Sulawesi, Indonesia. It is a fragment of ultramafic massif called East Sulawesi Ophiolite (ESO), which was emplaced during the Upper Cretaceous Time [12], [13]. Another research [14] compiled the study area's regional geology and identified two rock sequences that occupy the area studied: ophiolite rocks and Meluhu Formation. The ophiolite complex consists of peridotite, harzburgite, dunite, and serpentinite, while Meluhu Formation comprises sandstone, quartzite, black shale, red shale, phyllite, slate, limestone, and siltstone.

Five rock chip samples used in this study were taken from ex open-pit nickel laterite mine site in the Latowu village of Batuputih District, North Kolaka Regency, Southeast Sulawesi Province (Fig. 1). One drill core sample, including mineralized breccia, was provided by Exploration Department PT. Vale Indonesia Tbk, Soroako.

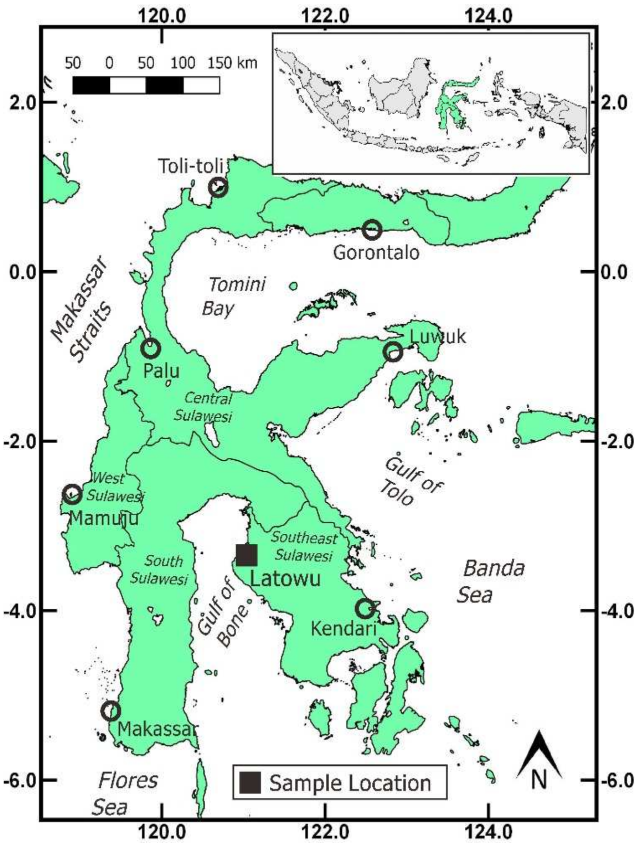


Fig. 1 Map showing Sulawesi Island and sample location

### B. Methods

After preparing polished-thin sections, optical microscopic analysis of rock samples was conducted employing a polarized light microscope (Nikon, Eclipse-LV100POL) in both reflected and transmitted light mode. Representative rock samples were comminuted using a jaw crusher followed by manual grinding using agate mortar to produce powder materials with a grain size less than 75µm for mineralogical and chemical analyses. The mineralogical composition of powder samples was determined using an X-ray diffractometer (Shimadzu, Maxima X-7000) with the following experimental conditions: voltage 40 kV, electric current 30 mA, scanning range 5 to 70° 2θ; scanning step 0.02° and scanning time 2°/minute. Data acquired in the form of diffractograms were further interpreted for mineral identification using the PDF-2 database and Impact Match! 3 (trial version).

Major element concentrations and some trace element content were obtained by X-ray fluorescence (XRF) spectroscopy. The chemical composition of minerals within the host rock and iron-rich minerals were analyzed utilizing the field emission - electron probe microanalysis (FE-EPMA, JEOL 8000 series, Tokyo, Japan). Microscopic and XRD analyses were performed at the Department of Geological Engineering, Hasanuddin University, whereas XRF and FE-EPMA analyses were carried at PT. Intertek Utama Services Jakarta and Faculty of Engineering, Hokkaido University, Sapporo, Japan, respectively.

## III. RESULTS AND DISCUSSIONS

### A. Petrology and Mineralogy of Ultramafic Host

The megascopic appearance of selected samples displays the texture of rocks showing medium to fine-grained with dark grey to reddish-brown in color and massive (Fig. 2A-C). The reddish-brown of the color is most likely hematite and locally is associated with silica. One sample displays an ultramafic breccia with subrounded and coarse grains (up to 2 cm in size), consisting of serpentinite, chromite, and magnetite (Fig. 2D). Hematite occurs as matrices within the ultramafic breccia.


Fig. 2 Chip samples of ultramafic rocks from Latowu showing brown to reddish-brown in color, indicating elevated concentration in iron oxides.

Photomicrographs of selected samples from Latowu ultramafic rocks are provided in Fig.3. Optical microscopic observation confirmed the extensive serpentinization of ultramafic rocks. Almost all *olivines* were replaced by serpentines forming network textures (Fig.3A and 3B). The early modal of olivine ranges between 60% and 90% by volume. The olivine relics are seen under the microscope showing grey using the plane-polarized light mode, but the color is changed into yellow or blue by crossed polar.

Similarly, orthopyroxene, likely enstatite, has also altered to serpentine forming batiste texture where the original shape is still maintained. The initial modal of orthopyroxene ranges from 10% to 30%. Orthopyroxene exhibits yellowish to pinkish under a microscope by crossed polar. Spinel is an accessory mineral with a quantity of up to 3%. Serpentinization of ultramafic rocks in the Latowu block shows uniform with the intensity ranges from 60% to 95%. Late-stage serpentine veins locally crosscut the primary serpentines, which replaced olivine and pyroxene. Magmatic spinels were crosscut by these veins as well (Fig.3B). Few samples containing orthopyroxene grains are locally transformed into talc and tend to alter primary crystals' periphery. The microscopic analysis indicated that the protolith of ultramafic rock in the Latowu area was dominated by harzburgite with less *dunnite*.

Chromite is present as a subhedral to anhedral grains, and the fractures developed in this phase are generally filled by serpentine. In mineralized ultramafic breccia, chromite and magnetite show subhedral to anhedral crystals acting as fragments. Serpentine, most likely lizardite, also presents as dominant fragments within the breccias. Matrices of this breccia are mainly composed of fine-grained serpentine and hematite (Fig. 3C).

Magnetite is commonly found as finely disseminated grains and discontinued thin veinlets. These crystals disperse in serpentine matrices (Fig. 3D). Styles of magnetite veinlets are dependent on the fracture development within the rock. Nickel sulfide phases, main pentlandite with rounded crystals, were locally observed.

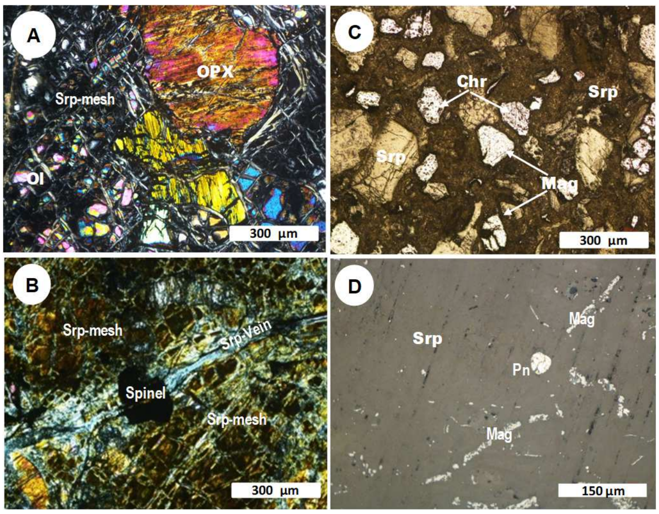


Fig. 3 Microscopic features of selected ultramafic rock samples from Latowu area. A and B are transmitted light with cross nicol; whereas C and D are reflected light mode. Ol=olivine, OPX=orthopyroxene, srp=serpentine, Chr=chromite, Mag=magnetite and Pn=pentlandite.

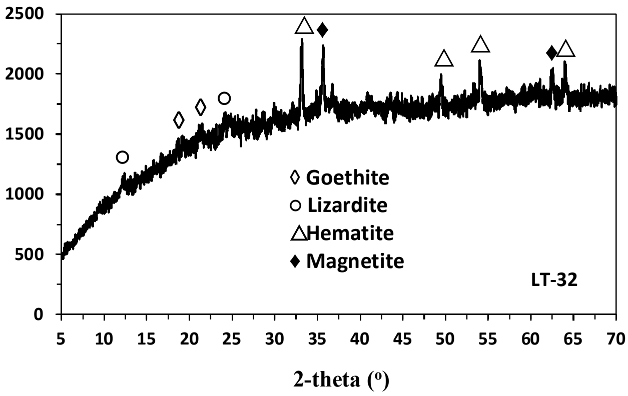


Fig. 4 Diffractogram of a mineralized ultramafic breccia

The XRD pattern of a mineralized ultramafic rock sample from Latowu is depicted in Fig. 4. It is indicated that lizardite is the predominant serpentine mineral identified within the analyzed powder rock sample. Reflection intensities with $d_{hkl}$ values around 7.29Å, 3.65Å, and 2.51Å are characteristics of lizardite. An additional peak occurring with $d_{hkl}$ value of 8.07Å could be assigned to chrysotile. Lizardite is an ample serpentine mineral having flatty crystal where the substitutions of $Fe^{3+}$ and $Ni^{2+}$ for $Mg^{2+}$ in its structure are possible, whereas chrysotile is less abundant and is characterized by tabular and fibrous crystals [15].

The occurrence of magnetite [$Fe_3O_4$] is indicated by the presence of reflection intensities with $d_{hkl}$ values of 2.53Å and 1.48Å. Hematite [$Fe_2O_3$] was also detected on the diffractogram which was marked by the maximum reflection intensity with $d_{hkl}$ value of 2.70Å. Other peaks appear with $d_{hkl}$ values of 1.84Å, 1.69 Å, and 1.45Å belong to hematite. Another iron oxide mineral identified within the ultramafic breccia based on XRD data was goethite [FeO.OH]. The presence of reflection intensities with $d_{hkl}$ values of 4.98Å and 4.18Å are characteristic peaks of goethite.

### *B. Whole Rock Geochemistry*

Major and some trace element compositions of the analyzed ultramafic rock samples are provided in Table I. Three principal oxides dominate the samples' chemical composition, namely $SiO_2$, MgO, and $Fe_2O_3$, with the sum of more than 80 wt% of the total oxides. The concentration of $SiO_2$ has lower values, ranging between 30.70 wt% and 42.82 wt%. Relatively low content of $SiO_2$ indicated that precursor minerals of serpentine were dominated by olivine. Similarly, MgO has a lower concentration ranging from 22.53 to 38.16 wt%. In contrast, $Fe_2O_3$ content displays wide range values with a minimum of 8.37 wt% and a maximum of 28.44 wt%. Except for sample LT-32, all samples exhibit low $Al_2O_3$ with values around 1 wt% or less. Other oxides such as CaO, $TiO_2$, MnO, and total alkali ($K_2O$ + $Na_2O$) show deficient grades (<1 wt% in total). The LOI content of the examined samples shows higher values ranging from 9.2 to 13.6 wt%.

The concentration of $Cr_2O_3$ lies within the range between 0.25 and 3.79 wt%; whereas Ni content has values ranging from 0.21 to 0.62 wt%. The concentration of Co has relatively narrow ranges (0.01 to 0.04 wt%) while Cu shows very low grade (<0.004 wt%).

TABLE I
WHOLE ROCK CHEMICAL COMPOSITION OF SELECTED SAMPLES FROM LATOWU AREA AS DETERMINED BY USING XRF

| Comp. (wt%) | Sample Codes | | | | | |
|---|---|---|---|---|---|---|
| | L-04 | L-09 | L-11B | L-12 | L-13 | L-32 |
| $SiO_2$ | 39.52 | 39.43 | 40.42 | 38.73 | 42.82 | 30.70 |
| $Al_2O_3$ | 0.83 | 0.86 | 0.29 | 0.14 | 1.01 | 3.98 |
| $TiO_2$ | <0.01 | 0.01 | 0.01 | <0.01 | 0.02 | 0.09 |
| MgO | 38.05 | 38.16 | 35.74 | 38.07 | 33.39 | 22.53 |
| $Fe_2O_3$ | 8.37 | 8.46 | 10.06 | 8.65 | 8.77 | 28.44 |
| MnO | 0.11 | 0.11 | 0.09 | 0.09 | 0.13 | 0.17 |
| CaO | 0.43 | 0.39 | 0.05 | 0.03 | 0.67 | 0.16 |
| $K_2O$ | <0.01 | <0.01 | <0.01 | <0.01 | <0.01 | 0.01 |
| $Na_2O$ | 0.04 | 0.04 | 0.03 | 0.03 | 0.04 | 0.05 |
| $P_2O_5$ | 0.01 | 0.01 | 0.01 | 0.01 | 0.01 | 0.02 |
| LoI | 11.20 | 11.60 | 12.50 | 13.60 | 12.10 | 9.20 |
| Tot.Oxide | **98.56** | **99.07** | **99.21** | **99.35** | **98.94** | **95.35** |
| Cr | 0.362 | 0.337 | 0.225 | 0.355 | 0.408 | 3.794 |
| Ni | 0.224 | 0.228 | 0.288 | 0.268 | 0.627 | 0.623 |
| Co | 0.011 | 0.010 | 0.012 | 0.012 | 0.011 | 0.046 |
| Cu | <0.002 | <0.002 | <0.002 | <0.002 | 0.004 | 0.003 |

### *C. Mineral Chemistry of Ultramafic Host*

Chemical composition determined by electron probe microanalysis (EPMA) of minerals composing in the ultramafic host is presented in Table II. It is shown that olivine contains higher MgO and FeO. Orthopyroxene (OPX) also has higher in MgO but lower in CaO as compared to clinopyroxene (CPX). Similarly, the concentration of FeO in OPX is higher as compared to CPX as well. The elevated concentration of CaO in CPX indicated that clinopyroxene could be assigned to the diopside [16]. Serpentine is higher in SiO2 than olivine but lower in MgO, indicating magnesium was more mobile than silicon during serpentinization.

Spinel, as an accessory mineral in ultramafic rock shows rich in $Al_2O_3$ with a value of 49.83 wt%. The ratio of $Al_2O_3$/MgO is 3.43, implying that some magnesium has been leached out from this mineral. The grade of $Cr_2O_3$ of spinel is low with about twice less than of $Al_2O_3$ content. Besides, to contain high FeO, magnetite also has a significant NiO and small quantities of $SiO_2$ and MgO.

TABLE II
SELECTED EPMA DATA (WT%) OF PHASES/MINERALS FOUND IN ULTRABASIC ROCK SAMPLES FROM LATOWU AREA

| Comp. (wt%) | Phases/Minerals | | | | | |
|---|---|---|---|---|---|---|
| | **Ol** | **OPX** | **CPX** | **Srp#** | **Spl** | **Mag** |
| $SiO_2$ | 40.98 | 52.43 | 50.71 | 46.72 | 0.29 | 2.26 |
| $TiO_2$ | 0.00 | 0.00 | 0.21 | 0.00 | 0.00 | 0.00 |
| $Al_2O_3$ | 0.00 | 3.87 | 4.04 | 0.00 | 49.83 | 0.00 |
| MgO | 48.61 | 33.79 | 14.49 | 44.01 | 14.54 | 1.78 |
| CaO | 0.00 | 1.12 | 26.91 | 0.00 | 0.00 | 0.00 |
| MnO | 0.29 | 0.46 | 0.24 | 0.00 | 0.01 | 0.00 |
| FeO | 9.52 | 7.38 | 2.31 | 8.79 | 13.01 | 94.04 |
| $Cr_2O_3$ | 0.00 | 0.95 | 1.11 | 0.00 | 22.04 | 0.00 |
| NiO | 0.61 | 0.00 | 0.00 | 0.49 | 0.28 | 0.62 |
| **Total Oxide** | **100.01** | **99.99** | **100.02** | **100.01** | **100.00** | **98.70** |

***Remark:*** *#anhydrous basis, Ol olivine,OPX orthopyroxene, CPX clinopyroxene, Srp serpentine, Spl spinel, Mag magnetite.*

### *D. Characteristics of Iron Mineralization*

Backscattered electron (BSE) images of iron-rich minerals containing selected ultramafic samples are provided in Fig. 5. It was shown that magnetite is the principal iron-bearing phases found in analyzed rock samples. Based on the textural relationship, magnetite in Latowu ultramafic rock can be classified into four different types: (i) as fragments, (ii) alteration rims, (iii) fine-grained disseminations, and (iv) thin veinlets.

Magnetite occurring as fragments in ultramafic breccia exhibits anhedral to subhedral crystals with grain sizes ranging from 50 to 1000 µm (Fig. 5A, B, and C). Magnetite is sometimes found to be associated with other ore minerals, mostly chromite. Both magnetite and chromite include spinel group minerals, and they appear to be the fragment components along with serpentinite grains within the breccia. Sulfide minerals, most likely pentlandite, and subordinate pyrite, were also observed in several grains. Some pentlandites have undergone progressive alteration. All fragments are set in serpentine and/or hematite matrices, which were cemented by iron oxides.

The alteration rim of magnetite occurs with the replacement of magmatic spinel mainly at the crystal edges and follow fracture orientations in spinel and/or crystal edges of pentlandite (Fig. 5A). With the increase of alteration intensity, magnesium in spinel easily releases into solution while the iron was relatively unresolved, leading to the enrichment of this element. A similar way occurs at pentlandite, where nickel and sulfur were oxidized.

Very fine grains disseminated of magnetite crystals were observed both in serpentinite and breccia. The grain size ranges between 0.5µm and 5µm (Fig. 5A; 5B and 5C). Thin veinlets show they discontinue and are commonly associated with serpentine, particularly lizardite. Magnetite also occurs as inclusion in spinel crystals.

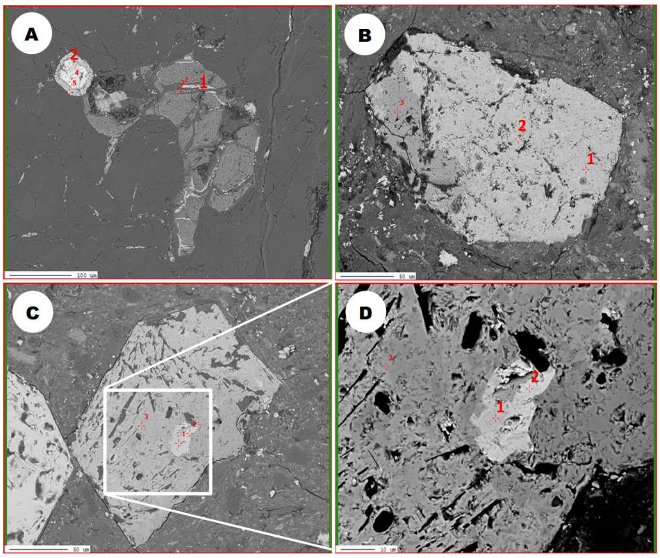


Fig. 5 Backscattered electron (BSE) images of iron-rich minerals associated with ultramafic rocks in the Latowu area. The iron-rich phase-filled fractures in spinel and serpentine and locally occur as an alteration rim of pentlandite (A). An iron-rich spinel set in hematite matrices (B). Euhedral spinel crystals occur as fragments in ultramafic breccia (C). An inset of one view in C (D).

Electron probe data of iron-riches mineral images depicted in Figure 5 are provided in Table III. The concentration of Fe ranges from 31.08 to 67.19 wt%; whereas Cr content of the samples ranges between 0.21 and 32.64 wt%. The grade of magnesium and silicon of the samples shows a low value (<3 wt%). Similarly, titanium and nickel also have very low grades (<0.1 wt%). The low content of titanium reveals Cr-spinel including in Ti-spinel peridotite. The aluminum concentration of the analyzed samples is very low (<1 wt%). These values contradict the spinel's Al2O3 content in ultramafic hosts, reaching up to 49.8 wt% (see Table II).

The wide range variation of Fe and Cr content within the mineral scale indicates different iron-bearing minerals. Based on FE-EPMA analysis, the iron-rich minerals were initially derived from the crystallization of Cr-spinel. During the alteration process (serpentinization or low-grade metamorphism), Fe was introduced into Cr-spinel, whereas Mg, Al, and Cr were diffused outward, leading to Fe mainly at the edges and/or fractures of Cr-spinel [17].

Further increase of fluid temperature causes the progressive penetration of fluid along the cracks and grain boundaries, leading to extensive alteration of Cr-spinel into ferrichrome and lately magnetite. Other elements such as Mg, Al, and Ni were also strongly depleted. Fe and Cr's difference mobility is confirmed by the binary diagram showing the strong negative correlation of these elements (Fig. 6) during the alteration process.

TABLE III
REPRESENTATIVE MICROPROBE DATA OF IRON-RICH MINERALS IN ULTRAMAFIC ROCKS FROM LATOWU AREA.

| Element | Spot No (wt%) | | | | | |
|---|---|---|---|---|---|---|
| | A-1 | A-2 | B1 | B2 | C1 | C2 |
| Ti | 0.02 | 0.00 | 0.12 | 0.02 | 0.15 | 0.04 |
| Fe | 58.81 | 67.19 | 31.08 | 64.55 | 45.25 | 62.44 |
| Cr | 1.42 | 0.21 | 32.64 | 3.70 | 19.99 | 6.60 |
| Si | 2.82 | 0.29 | 0.16 | 0.13 | 0.02 | 0.04 |
| S | 0.00 | 0.02 | 0.00 | 0.01 | 0.00 | 0.00 |
| Al | 0.10 | 0.02 | 0.37 | 0.03 | 0.91 | 0.12 |
| Mg | 2.10 | 0.32 | 1.27 | 0.03 | 1.00 | 0.43 |
| O | 26.34 | 26.13 | 28.48 | 29.69 | 27.72 | 27.70 |
| Ni | 0.10 | 0.09 | 0.13 | 0.04 | 0.12 | 0.03 |
| **Total** | **91.714** | **94.267** | **94.254** | **98.193** | **95.161** | **97.395** |

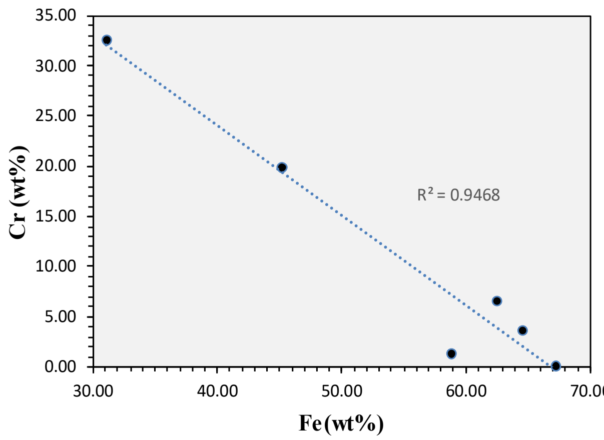


Fig. 6 Binary diagram showing the strongly negative correlation between Cr and Fe of the iron-rich minerals.

## *E. The Origin of Magnetite*

Magnetite in the Latowu area is hosted in highly serpentinized ultramafic rocks. Microscopic observation showed that olivine is the predominant primary minerals with subordinate pyroxene. Spinel presents as an accessory mineral. This suggests that the protolith of these ultramafic rocks are harzburgite with less *dunnite*. Mostly olivine and pyroxene have been altered to serpentine.

Formation of iron oxide, mostly magnetite during serpentinization of ultramafic rocks might be the result of oxidation of ferrous iron ($Fe^{2+}$) into ferric iron ($Fe^{3+}$) in olivine and/or pyroxene [18]. Some possible reactions were described to propose the formation of magnetite during serpentinization of ultramafic rocks. In a low-temperature environment (50 to 300ºC), lizardite is the predominant serpentinization product [19].

Hydration of olivin is the primary process in ultramafic rocks to generate serpentine, brucite, magnetite, and hydrogen [20] according to one or more of the following reactions:

Olivine + $H_2O$ → serpentine + magnetite + $H_2$ (1)
Olivine + $H_2O$ → lizardite + magnetite + brucite + $H_2$ (2)
Olivine + $H_2O$ + $O_2$ → serpentine+ brucite + magnetite (3)

It can be seen that reactions 1 and 2 produce hydrogen through the breakdown of H2O, leading to the strong reduction condition of fluids during serpentinization [21]. The relatively low content of CaO (mostly < 1 wt%) suggests that orthopyroxene was initially present in ultramafic rocks. Similarly, the concentration of $Al_2O_3$ was also low (mostly <2 wt%). This condition may promote the formation of magnetite. In contrast, the significant amounts of aluminum and silica released by primary minerals, such as clinopyroxene and spinel during serpentinization, may humper magnetite production. The highest value of magnetic susceptibility of samples (up to 0.043 SI, data not shown) is consistent with the high serpentinization degree of rock. However, those parameters do not show a good linear correlation because the multistage processes have taken place during serpentinization such that the rate of magnetite production increases with the serpentinization degree [22]

In the case of alteration rim of spinel, reference [23] suggested that the magnetite rim formation is related to the dissolution-precipitation process where Mg and Al were depleted while Fe was enriched relative to the core. Magmatic Al-spinel underwent re-equilibrium in the oxidizing water-rich environment after the serpentinization process [24], leading to the exchange reaction of $MgAl_2SiO_4$ by Cr-magnetite.

The occurrence of ultramafic breccia is not clear, but it might be included as hydrothermal breccia because some fragments contain oxide ores (magnetite and chromite) and contain Ni-Fe alloy phases. As a matrix component of breccia, hematite's presence is likely to transform magnetite products [25].

A relatively higher grade of Ni found in two samples reaches up to 0.62 wt% (see Table I) indicate that the enrichment of nickel in serpentinized ultramafic rocks could be related to the formation of sulfide minerals such as pentlandite and awaruite which follow the serpentinization. Ni in olivine's removal during serpentinization might cause Ni-rich minerals precipitation depending on sulfur content in the fluid [26].

## *F. The Implication for Iron Ore Beneficiation*

Result of whole-rock chemical analysis exhibit that one analyzed sample contains 28.44 wt% $Fe_2O_3$. The ore used for iron making in blast furnace should contain at least 60%. The iron ore from Latowu can be categorized as low-grade ore; therefore, it is not suitable for direct feeding in blast furnace operation applied in steel production. Some methods can be implemented in upgrading the iron value, such as magnetic separation, gravity concentration, reduction roasting, and a combination of these. However, the selection of proper beneficiation strategies depends on the mineralogical properties of the ore, including magnetic mineral, grade, texture, and impurities [27], [28], [29], [30].

In the case of Latowu iron ore sample, the domination of magnetite as an iron-bearing mineral indicate that magnetic separation is a suitable way of upgrading the iron value. However, the ore texture shows fine-grained and disseminated, which means that the ore should be comminuted before separation to liberate the iron-rich phases from gangue minerals, mainly serpentine.

## IV. Conclusion

The occurrence of iron mineralization hosted in serpentinized ultramafic rocks, originated from Latowu block, has been assessed. Based on the results and discussion regarding the textural relationship, mineral properties, and chemical composition for both host rock and ore minerals, some conclusions can be drawn as follows: The ultramafic rocks of Latowu block have been altered into serpentine with moderate to complete degree forming mesh texture after olivine and locally forming batiste texture after pyroxene. Lizardite is the most common serpentine mineral formed, and it is followed by chrysotile. Both minerals are most likely derived from olivine alteration with local pyroxene.

Iron mineralization represented by magnetite formation was derived from the alteration of Cr-spinel and newly form magnetite crystals following the serpentinization of ultramafic rocks. Factors that might promote magnetite production during serpentinization are mineralogical and chemical composition of protolith, fluid chemistry, and temperature. Based on the mineral properties of iron-bearing minerals, magnetic separation can be a potential method in upgrading the iron value.

## Acknowledgment

This work was financially supported by the Directorate of Research and Community Services (DRPM), Directorate General of Higher Education through Decentralization Grant managed by LP2M of Universitas Hasanuddin under University Applied's scheme Research Excellence or PTUPT, contract No. 1578/UN4.21/PL.00.00/2018. The authors gratefully acknowledge Mr. Absar of the Exploration Department, PT. Vale Indonesia Tbk for providing drill core samples and Mr. Sukadi of PT. Kurnia Mining Resources for his assistance during the fieldwork. Thanks, are also directed to Dr. Kenzo Senematsu of AIST Tsukuba, Japan, for helping in EPMA analysis of host rock samples.

## References

[1] H. Van Oss, "Iron Ore" (in Mineral Commodity Summaries, USGS), 2018.

[2] Sufriadin, S. Widodo and M. Trianto, "Beneficiation of lateritic iron ore from Malili Area, South Sulawesi, Indonesia using magnetic separator", *IOP Conf. Ser. Mater.Sci.Eng,* Vol.619, pp. 12-17, 2019.

[3] K.K. Chatterjee, "Uses of metals and metallic minerals", New Age International Publishers, New Delhi, 2007

[4] S. Carbonin, S. Martin, S. Tumiati, P. Rossetti, "Magnetite from the Cogne serpentinites (Piemonte ophiolite nappe, Italy). Insights into seafloor fluid–rock interaction", *European Journal of Mineral,* vol. 27, pp. 31 – 50, 2015.

[5] L. Toppolo, P. Nimis, S. Martin, S. Tumiati and W. Bach, "The Cogne magnetite deposit (Western Alps, Italy): A Late Jurassic seafloor ultramafic-hosted hydrothermal system?, *Ore Geology Reviews,* Vol.83, pp. 103-126, 2016.

[6] H.A. Gahlan, S. Arai, H.A. Ahmed, Y. Ishida, Y.M. Abdel Aziz, A. Rahimi, "Origin of magnetite veins in serpentinite from the Late Proterozoic Bou-Azzer ophiolite, Anti-Atlas, Morocco: An implication for mobility of iron during serpentinization", *Journal of African Earth Science*, vol. 46, pp. 318-330, 2006.

[7] M.Z. Khedr, and S. Arai, "Composite origin of magnetite deposits hosted in Oman peridotites: Evidence for iron mobility during serpentinization", *Ore Geology Review*, vol. 101, pp.180-198, 2018.

[8] Z.B. Liu, J.C.Li, T. Zhao, Y. Zong, G.L. Yuan, Y.Lin, H.S. Shao, "Serpentinisation and magnetite formation in the Angwu ultramafic rocks from the central Bangong–Nujiang suture zone, Tibetan Plateau", *Geology Journal*, pp.1 – 17, 2019.

[9] F. Hodel, M. Macouin, A. Triantafyllou, J. Carlut, J. Berger, S. Rousse, N. Ennih, R.I.F. Trindade, "Unusual massive magnetite veins and highly altered Cr-spinels as relics of a Clrich acidic hydrothermal event in Neoproterozoic serpentinites (Bou Azzer ophiolite, Anti-Atlas, Morocco)", *Precambrian Research*, vol 300, pp. 151 – 167, 2017.

[10] S. Kai, L. QingSong, J. ZhaoXia, D. SongQi, "Mechanism of magnetic property changes of serpentinites from ODP Holes 897D and 1070A, *Science China Earth Science*, vol.58, pp. 815-829, 2015.

[11] R. Rafianto, F. Attong, A. Matano, and E.S. Noor, "The serpentine-related nickel sulfide occurrences from Latowu, SE Sulawesi: a new frontier of nickel exploration in Indonesia", *Majalah Geologi Indonesia,* vol. 27, pp. 87-107, 2012.

[12] C. Monnier, J. Girardeau, R.C. Maury and J. Cotten, "Back-arc basin origin from the East Sulawesi ophiolite", *Geology,* vol. 23, No.9, pp. 851 – 854, 1995.

[13] A. Kadarusman, S. Miyashita, S. Maruyama, C.D. Parkinson, and A. Ishikawa, "Petrology, geochemistry and paleogeographic reconstruction of the East Sulawesi Ophiolite, Indonesia", *Tectonophysics,* vol. 392, pp. 55 – 83, 2004.

[14] E. Rusmana, Sukido, D. Sukarna, E. Haryono, and T.O. Simandjuntak, T.O., "Geological map of Lasusua-Kendari Quadrangle of Sulawesi", Geological Research and Development Center, Bandung, 1993.

[15] O.R.D.R. Carmignano, S.S. Vieira, P.R.G. Brandao, A.C. Bertoli, R.M. Lago, "Serpentinites: Mineral Structure, Properties and Technological Applications", J. Braz. Chem. Soc., Vol. 31. pp. 2-14, 2020.

[16] W.A. Deer, R.A. Howie, J. Zussman, "An introduction to rock forming minerals", Prentice Hall, New York, 1992.

[17] I.M. Bhat, T. Ahmad, D.V.S. Rao, "Alteration of primary Cr-spinel mineral composition from the Suru Valley ophiolitic peridotites, Ladakh Himalaya: Their low-temperature metamorphic implications", *J. Earth Syst. Sc.* Vol. 128:188, pp. 1 – 14, 2019.

[18] R. Huang, C.T. Lin, W. Sun, X. Ding, W. Zhan, J. Zhu, "The production of iron oxide during peridotite serpentinization: Influence of pyroxene", *Geoscience Frontier*, vol.8, pp. 1311-1321, 2017.

[19] B.W. Evans, "Lizardite versus antigorite serpentinite: Magnetite, hydrogen, and life (?)", *Geology,* vol. 38, pp.879-882, 2010.

[20] T.M. McCollom, F. Klein, B. Mackowitz, T.S. Barquo, W. Bach, A.S. Templeton, "Hydrogen generation and iron partitioning during experimental serpentinization of an olivine–pyroxene mixture", *Geochimica et Cosmochimica Acta*, vol. 282, pp. 55 – 75, 2020.

[21] T.M. McCollom, and W. Bach, "Thermodynamic constraints on hydrogen generation during serpentinization of ultramafic rocks", *Geochemica et Cosmochimica Acta*, vol. 73, pp. 856-875, 2009.

[22] O. Oufi, and M. Cannat, "Magnetic properties of variably serpentinized abyssal peridotites", *Journal of Geophysical Research*, vol. 107, pp. 3 – 19, 2002.

[23] K.L. Kimball, "Effect of hydrothermal alteration on the compositions of chromian spinels", *Contrib. Mineral Petrol*. vol.105, pp. 337 – 346, 1990.

[24] M. Mellini, C. Rumori, C.Viti, "Hydrothermally reset magmatic spinels in retrograde serpentinites: formation of ''ferritchromit'' rims and chlorite aureoles, *Contrib Mineral Petrol*. vol. 149, pp. 266 – 275, 2005.

[25] T. Otake, D.J. Wesolowsky, L.M. Anovits, L.F. Allard, and H. Ohmoto, "Experimental evidence for non redox transformations between magnetite and hematite under $H_2$-rich hydrothermal conditions", *Earth and Planetary Science Letters*, vol. 257, pp. 60 – 70, 2007.

[26] M. Sciortino, J.E. Mungal, and J. Moinonen, "Generation of high-Ni sulfide and alloy phases during serpentinization of dunite in the Dumont Sill, Quebec". *Economic Geology*, vol.110, pp. 733-761, 2015.

[27] S.P. Suthers, V. Nunna, A. Tripathi, J.Douglas and S. Hapugoda, "Experimental study on the beneficiation of low-grade iron ore fines using hydrocyclone desliming, reduction roasting and magnetic separation", *Mineral Processing and Extractive Metallurgy (Trans. Inst. Min. Metall. C)*, vol. 123, No.4, pp. 212-227, 2014.

[28] S. Patra, A. Pattanaik, A.S. Venkatesh, R. Venugopal, "Mineralogical and Chemical Characterization of Low Grade Iron Ore Fines from Barsua Area, Eastern India with Implications on Beneficiation and Waste Utilization', *Journal of Geological Society of India*, vol. 93, pp. 443 – 456, 2019.

[29] H. Akbari, M. Noaparast, S.Z. Shafaei, A. Hajati, S. Aghazadeh, H. Akbari, "A Beneficiation Study on a Low Grade Iron Ore by Gravity and Magnetic Separation", *Russian Journal of Non-Ferrous Metals*, Vol. 59, No. 4, pp. 353–363, 2018.

[30] M. Altiner, "Upgrading of iron ores using microwave assisted magnetic separation followed by dephosphorization leaching", *Canadian Metallugical Quarterly*, Vol. 58, pp. 445 – 455, 2019.